

12

Theoretical Analysis of Culture Growth in Flat-Plate Bioreactors: The Essential Role of Timescales

Y. Zarmi, G. Bel, and C. Aflalo

Jacob Blaustein Institutes for Desert Research, Ben-Gurion University of the Negev, Midreshet Ben-Gurion, Israel

Abstract

Qualitative characteristics of biomass production in ultrahigh density algal bioreactors with a small optical path (specifically, thin flat-plate reactors) are analyzed and explained in terms of models, which combine the random motion of cells across the optical path with simple models for the photosynthetic process. Characteristics of different models at extreme densities are compared with existing data. An analogy between flashing light illumination and the light regime experienced by the randomly moving cells provides basic insight into the important role of timescales in reactor performance. The emergence of an optimal culture density (OCD), at which the volumetric and areal production rates are maximal, is understood in simple terms. While higher density implies an increase in the number of photosynthesizing cells, it leads to narrowing of the illuminated (photic) zone, hence to a decrease in the time spent by these cells in the photic zone. When the time spent by cells in the photic zone is longer than the time needed to collect the photons required for the photosynthetic process, the addition of cells increases the volumetric production rate. When the time spent by cells in the illuminated zone falls below the time needed for the collection of photons, the volumetric production rate is decreased. The combined effects of changes in density are the cause of the emergence of an OCD. At the OCD, the time spent by cells in the thin illuminated layer of the culture and the time needed for the collection of the photons required for the photosynthetic process coincide.

Keywords algal bioreactors; ultrahigh densities; small optical path; cell random motion; synchronization of timescales

12.1 INTRODUCTION

12.1.1 The issues addressed in this chapter

In traditional pond or raceway bioreactors, culture densities and areal production rates are low, and the optical path (OP, the distance that light traverses, typically,

the depth of the reactor, throughout which cells move) hardly affects biomass production rates at all. The situation is different in thin flat-plate bioreactors, where production rates and culture densities are appreciably higher than in conventional reactors, and are strongly dependent on the OP.

The number of experiments that have been performed on thin flat-plate bioreactors is small. Much worse, at present, there is hardly any precise knowledge of the **dynamical** parameters, that is, timescales, reaction-rate constants, etc., which characterize the photosynthetic process. Hence, it is impossible to rigorously test hypotheses or quantitative models that offer explanations for the observations. Still, the experimental results obtained in such reactors offer exciting possibilities for new insight into, and raise questions about, some characteristics of the photosynthetic process.

This chapter is dedicated to raising open questions regarding the quantitative characteristics of the photosynthetic process, as well as the physical motion of algal cells in the culture, all of which affect culture productivity. In particular, the aim is to demonstrate that a main cause for the phenomena observed in thin flat-plate reactors is the approximate synchronization between some of the timescales that characterize physical cell motion in stirred reactors and the timescales that characterize the photosynthetic process.

The remainder of this section is dedicated to a review of experimental results in conventional and thin flat-plate bioreactors. Section 12.2 is devoted to the description of thin flat-plate bioreactors and to a qualitative discussion of the expected characteristics of productivity, showing the important role of algal cell random motion across the OP. Section 12.3 presents the qualitative features of the mathematical models that have been employed. Section 12.4 presents a discussion of the effect of timescales on the productivity of a single cell when it is exposed to light flashes with fixed flash- and dark-interval durations and a constant light intensity during each flash. The results of this simple model provide a qualitative picture for what is to be expected from the more complicated model, in which cell random motion is taken into account. Numerical results, based on the models discussed in Section 12.3 are presented in Section 12.5. Section 12.6 presents some open questions.

12.1.2 Conventional versus thin flat-plate bioreactors

The OP (optical path) in traditional pond or raceway bioreactors for unicellular algae is well over 10 cm. It has a negligible, if any, effect on the biomass production rate (Richmond et al., 1990; Sukenik et al., 1991). Culture densities in traditional reactors are low, of the order of 1 g dry-weight per liter, and so are the volumetric production rates, for example, for an OP of 10 cm, they are of the order of 0.01 g L⁻¹ h⁻¹ (Richmond, 2004; Schenk et al., 2008). Finally, the exploitation of light intensities substantially higher than one sun is impractical, owing to the strong effect

of photoinhibition. These observations can be understood in terms of a simple steady-state picture because the time required for algal cells to cross the OP is much longer than the timescales that characterize the photosynthetic process. In common tubular reactors, with tube diameter typically 10 cm and over, again, one does not expect a strong effect of tube diameter on productivity.

In thin flat-plate bioreactors (OP of the order of 1 cm), areal production rates and culture densities are appreciably higher than in conventional reactors (Gitelson et al., 1996; Hu et al., 1996, 1998a; Richmond, 1996, 2000, 2003, 2004a, 2004; Richmond & Hu, 1997; Richmond & Zou, 1999; Zou & Richmond, 1999, 2000; Richmond & Zhang, 2001; Richmond et al., 2003). For example, in experiments on *Spirulina platensis* in inclined flat-plate reactors facing the sun, the optimal cell density (OCD, the density at which the volumetric biomass production rate is maximal) increased approximately by one order of magnitude (from 1 to 10–20 g L⁻¹), and the maximal volumetric growth rates increased from 0.024 to 0.31 g L⁻¹ h⁻¹ when the OP reduced from 10.4 to 1.3 cm (Hu et al., 1998a). Moreover, productivity consistently increased as incident light intensity was raised (Hu et al., 1998a, 1998b), even up to several suns. No signs of saturation were observed as light intensity was raised (except at the highest intensity of four suns), to the extent that the effect of photoinhibition does not seem to be significant.

12.1.3 Some relevant timescales

A schematic view of a thin flat-plate bioreactor is shown in Figure 12.1. Light penetrates from the sides, and cells move back-and-forth across the reactor thickness from darkness

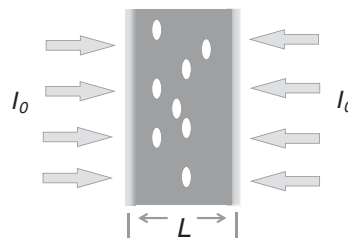


Figure 12.1. Cross-sectional view of narrow side of flat-plate bioreactor illuminated on both sides. I_0 , incident light intensity; L , reactor thickness. At ultrahigh culture density, most reactor volume is dark; only a narrow layer ("photic" zone) on either side is illuminated. Rising air bubbles generate turbulent motion of fluid.

in the bulk of the volume, to a thin photic zone, with thickness of the order of 1 mm or less.

Consider a flat-plate bioreactor, in which culture density is of the order of 10 g L^{-1} . Depending on the mixing rate induced in the culture due to turbulent fluid flow, the typical time spent by cells in the thin illuminated layer (the photic zone) may be of the order of 1–10 ms, which is of the order of the time a reaction center needs in order to collect the number of photons required for one photosynthetic cycle. Similarly, the crossing time of cells from the dark midpoint of a 1 cm thick reactor, illuminated on both sides, to the illuminated layers near its walls is of the order of tens to several hundreds of milliseconds. The effective turnover time for one cycle of the photosynthetic unit was estimated years ago (in phytoplankton, at relatively low radiation levels) to be of the order of 3–10 ms (Falkowski et al., 1985; Dubinsky et al., 1986). Photon energy loss processes, which compete with the photosynthetic process, occur at timescales ranging from nanoseconds (which may be viewed as instantaneous and affecting the effective quantum efficiency) up to several milliseconds (Tyystjärvi & Vass, 2004; Goltsev et al., 2005; Cogdell et al., 2008; Goltsev et al., 2009).

12.2 FLAT-PLATE BIOREACTORS – QUALITATIVE EXPECTATIONS

12.2.1 Reactor geometry and random cell motion

A cross-sectional view of a flat-plate bioreactor is shown in Figure 12.1. The width and height of the reactor are dictated by experimental or production process limitations. Its thickness (L , the optical path, OP) is of the order of one to a few centimeters. Light is shone on one or both flat walls. Air bubbles fed at the bottom generate turbulent motion in the fluid (Sato & Seguchi, 1975, 1981; Michiyoshi & Serizawa, 1986; Pan et al., 1999; Pflieger et al., 1999; Deen et al., 2001; Sokolichin et al., 2004; Al Issa & Lucas, 2009). Owing to this turbulent flow, cells perform random motion throughout the reactor. While there is no good theory for this random motion, a phenomenological description exists (Sato & Seguchi, 1975, 1981), according to which, fluid elements, hence, anything in suspension in the fluid, move randomly; their motion is similar to the Brownian motion of molecules.

The parameter that characterizes a random walk is the diffusion coefficient, D , which determines the average spread in time of the randomly moving objects (molecules or algae). Denoting by x the distance a randomly walking object has travelled in one dimension during a time span

t , the average of the square of the distance travelled, $\langle x^2 \rangle$, grows linearly with time:

$$\langle x^2 \rangle = 2Dt \quad (12.1)$$

For random motion inside a finite interval, Equation 12.1 is a valid approximation as long as the randomly moving object is not too close to the walls, and only for times shorter than the average crossing time of the whole interval.

There is a difference of orders of magnitudes between molecular Brownian motion and the macroscopically observable random motion of algal cells in a reactor owing to turbulence induced by mixing. In the Brownian motion of small molecules in still water, D has values of the order of $10^{-5} \text{ cm}^2 \text{ s}^{-1}$, whereas, for algae in mixed suspension, D has values of the order of $1 \text{ cm}^2 \text{ s}^{-1}$ owing to the turbulent motion of the fluid. This means that, in one second, on average, an oxygen molecule moves in still water a distance of the order of 0.005 cm, while an alga cell traverses an average distance of the order of 1 cm. D provides a measure of the mixing rate in the culture.

12.2.2 Cell random motion and light regime

Moving randomly through the reactor, cells are exposed to randomly varying light intensities. At high culture densities, the light intensity falls off rapidly into the depth of the reactor (roughly exponentially); it is appreciable only in the thin photic zone. Consequently, the light regime, to which the cells are exposed, **mimics light flashes**. The duration of flashes varies randomly. The average of flash duration is of the order of the average time a cell spends in the photic zone. The time intervals of motion between flashes (in the dark part of the reactor) also vary randomly. Their average is the average time required to cross the dark portion of the reactor. As the width of the dark portion is close to the total thickness of the reactor (the OP), the average dark-time interval is of the order of the time required on average for a cell to cross the entire reactor width.

12.2.3 Volumetric production rate – effects of culture density and cell random motion

In the absence of cell motion, beyond biological considerations (e.g., the need for an effective mass transfer of reactants), the volumetric production rate is expected to rise up to a constant value at high densities (Gebremariam, 2008; Greenwald, 2010; Gebremariam & Zarmi, 2012). This is **independent** of the particular model of the photosynthetic process. The experimental observation in stirred reactors that, at a given incident light intensity, the volumetric production rate rises as a function of the density at

low densities, reaches a maximum (at the OCD) and then decreases at higher densities, can be qualitatively understood as follows.

At **low densities**, for which the average light intensity throughout the reactor is close to the incident intensity, the specific production rate (per catalytic unit) is highest and has a weak dependence on density in that range. Hence, despite the attenuating effect of density on the light intensity, the increase of density leads to a rise in the volumetric production rate. On the other hand, at **very high culture densities**, the specific production rate sharply drops as density is increased, to the extent that an increase in catalytic units cannot prevent the decrease in the volumetric production rate. The rise at low densities and the decrease at high densities dictate the existence of an OCD.

In this chapter, we discuss the combined effect of cell random motion and different approaches to the modeling of the photosynthetic process. In two of the models considered here, the explanation proffered above for the experimental results is realized, whereas one model fails to do so.

Clearly, an increase in culture density (i.e., catalytic units) is expected to contribute to the volumetric production rate. On the other hand, increasing the density leads to a sharper decrease of light intensity into the depth of the reactor. As a result, the thickness of the photic zone is reduced. Consequently, the time a cell explores the photic zone in its random motion is shortened. The combined effect of the increase in the number of catalytic units and of the shorter time spent in the photic zone is shown to be the source for the emergence of an OCD.

12.2.4 OP length and productivity

The synchronization between the timescales related to cell motion and the timescales that characterize the photosynthetic process affects productivity. Once a cell has collected the required number of photons and leaves the photic zone, it wanders throughout the dark portion of the reactor volume (which is most of the reactor as the photic layer is thin). Consider again an OP of 1 cm in a reactor that is illuminated only on one side. Assuming a diffusion coefficient, D , of $1 \text{ cm}^2 \text{ s}^{-1}$, the time spent by a cell moving randomly through the dark volume of the reactor is of the order of 300–500 ms. This time is **much** longer than the time span (of the order of 5–10 ms) that the photosynthetic apparatus needs in order to convert the energy of photons just absorbed into chemical energy, and, eventually, into biomass. Hence, some time is wasted while cells wander throughout the dark volume; they have long completed a photosynthetic cycle and are still wandering in the dark portion before they reach the photic zone. It, therefore, pays to reduce the OP as much

as possible in order to shorten the time spent in the dark portion of the reactor. However, mechanical limitations prevent the reduction of reactor thickness much below 1 cm. Instead, one may irradiate the reactor on both sides. The productivity then grows by a factor of 2 relative to one-side illumination. This qualitative statement has been observed experimentally (Hu et al., 1996; Richmond, 1996, 2000, 2003, 2004a, 2004).

12.2.5 Extreme culture densities

Around the OCD, the volumetric production rate is insensitive to small density changes. At **very low culture densities**, the light intensity is close to uniform throughout the reactor, so that cells at all locations are exposed to roughly the same intensity. Consequently, they all produce biomass at roughly the same rate. Hence, as density is increased, the contribution of additional catalytic units overcomes the effect of light attenuation, resulting in an increase of the volumetric productivity toward maximal productivity, which occurs at the OCD.

At **culture densities significantly higher than the OCD**, the light intensity becomes the major limiting factor. Since the photic zone is very thin, a reaction center cannot collect the required number of photons in one visit to the photic zone and may have to visit there several times. In between visits, the cell moves randomly in the dark portion of the reactor, losing some or all of the (insufficient) collected photon energy. Consequently, the specific production rate becomes low; the volumetric culture productivity drops below the maximal value at the OCD.

The increase with density in the volumetric production rate at low densities and its decrease at high densities leads to the emergence of the OCD, at which the volumetric production rate is maximal. This observation agrees qualitatively with experimental observations.

12.2.6 Increasing light intensity and photoproductivity

At very low culture densities, light intensity throughout the reactor is close to the incident intensity. As one increases the latter, the effect of photoinhibition becomes more pronounced. However, at higher densities, the photic zone becomes narrower, and the time spent in it is short. Hence, the probability of being hit by more photons than required for one photosynthetic cycle diminishes. This effect is especially pronounced at densities around the OCD and beyond. In addition, as the incident light intensity is increased, a reaction center needs less time to collect the same number of photons for one photosynthetic cycle. Hence, the photic zone must become narrower. This means that the OCD has

to grow. Thus, one expects the OCD to grow as light intensity is increased.

Finally, owing to the short time the cells spend in the photic zone, photoinhibition is not expected to affect the production process significantly. Consequently, productivity is expected to increase as the light intensity is raised since more cells are efficiently collecting photons (higher OCD, with undamaged efficiency). Such an increase is observed in the experimental data.

12.3 MODELS FOR PHOTOSYNTHESIS BY RANDOMLY MOVING CELLS

Modeling of productivity in a reactor must account for the characteristics of the photosynthetic process and the light regime. Owing to the attenuation of light intensity throughout the reactor, the light regime is determined by cell motion. In our models, we have incorporated two ingredients: cell random motion and a simplified description of the photosynthetic cycle. Light attenuation is assumed to be a function of culture density. Hence, we present results for bioproductivity as a function of two independent variables: incident light intensity and culture density.

Cell motion is determined by hydrodynamic factors, such as mixing rate and the physical properties of the fluid and the cells. In our models, the random motion of the cells is fully characterized by the diffusion coefficient, D , which is assumed to be independent of culture density. The motion of the cells parallel to the reactor walls is of no consequence for biomass productivity. Only their motion perpendicular to the walls, that is, along the OP, is relevant. Hence, cell motion is modeled as a random walk in one dimension only, along the OP (see Eq. 12.1).

The photosynthetic process in a cell is affected by the conditions prevailing in the reactor, that is, the local light intensity. We assume that all photon-absorption rates are linear in light intensity. However, we do not account for the physiological acclimation of cells to changes in light intensity in terms of light processing efficiency of the catalytic system.

At ultrahigh culture densities, the light intensity falls off rapidly from its incident value into the depth of the culture. In our calculations, we have assumed an exponential fall off. Namely, given the incident light intensity, I_0 , the intensity at a distance x from the wall into the culture is given by

$$I(x) = I_0 e^{-\mu x} \quad (12.2)$$

The attenuation coefficient, μ , depends on culture dry-weight density, ρ_{DW} , or on chlorophyll density, ρ_{Chl} . In the numerical results presented here, it has been assumed (due

to the lack of precise knowledge) that μ is not affected by the light regime and is related approximately to either density by a linear relationship:

$$\mu \approx \alpha \rho_{DW} \approx \varepsilon \rho_{Chl} \quad (12.3)$$

where α and ε are the corresponding specific attenuation coefficients.

Two approaches were employed for the description of the photosynthetic cycle. One approach considers the dynamics of a single reaction center operating in a sequential mode: photon collection accompanied by photon energy loss, followed by catalysis, during which no photon collection occurs. In the second approach, the photosynthetic process is described by phenomenological multi-step rate equations. These equations describe the dynamics averaged over a large ensemble of centers (there are about 10^5 – 10^6 reaction centers in a cell; see Falkowski et al., 1981).

Both approaches lead to the same qualitative predictions for the dependence of productivity on culture density and on light intensity. This indicates that, with timescales of the photosynthetic process being what they are, the **light regime** is the dominant factor in reactor performance. Owing to the random motion, approximate synchronization between the average time spent by cells in the photic zone and the timescales of the photosynthetic process is a major factor in determining productivity. In all model calculations, the light intensity, I , is measured in photons $RC^{-1} s^{-1}$.

12.3.1 Model I – sequential collection reaction

Assuming that, in a rough approximation, the biomass production rate is proportional to the average rate at which a single catalytic unit (referred to as “reaction center,” composed of two photosystems) exploits photons for generating chemical energy, the model counts the average number of photosynthetic cycles that a single reaction center undergoes per unit time while the cell moves randomly throughout the reactor (Gebremariam, 2008; Greenwald, 2010; Gebremariam & Zarmi, 2012). The cycle is treated in a “black box” description, characterized by three timescales:

1. T_d , the time span, during which, after having collected the number of photons required for one photosynthetic cycle, a reaction center is busy converting absorbed photon energy into chemical energy and is unavailable for the absorption of additional impinging photons. Based on previous works (Falkowski et al., 1985; Dubinsky et al., 1986), T_d varies in the range 1–10 ms.

2. T_e , a timescale characterizing photon energy loss (mostly, owing to decay processes, in which absorbed photon energy is lost as radiation, often long-wave radiation). If a reaction center does not collect the required number of photons (we assume 8) during a time span equal to T_e , then all collected photon energy is lost and a new cycle begins. T_e is estimated to be of the order of 1–10 ms (Tyystjärvi & Vass, 2004; Goltsev et al., 2005, 2009; Cogdell et al., 2008).
3. T_{coll} , the time needed for collecting the number of photons required for one cycle (say, 8). T_{coll} is not constant; rather, it varies randomly owing to the varying light intensity that the cell encounters while performing its random walk. Clearly, T_{coll} depends on antenna size.

A variant of this model, in which photon energy loss does not occur in a sharp cut-off manner as above, but through a decay process, yields qualitatively and quantitatively similar results. In this variant, while photons are collected during some time interval Δt , the fraction of collected energy that is lost is given by an exponential decay factor of the form $\exp(-\Delta t/T_e)$. Results of this variant are presented in Section 12.5.4.

In this model, bioproductivity is measured by the average number of photosynthetic cycles completed by a reaction center per second.

12.3.2 Model II – ensemble-averaged kinetics

In this approach, the photosystems involved in the photosynthetic cycle are considered as a single catalytic unit. The photosynthetic process is decomposed into elementary steps: (i) photon absorption, yielding reversible excitation of the photosystem complex to an active state; (ii) electron transfer catalyzed by the activated complex; (iii) inactivation by excess photon absorption, yielding an irreversibly inhibited state; and (iv) repair of the latter back to the ground state. Note that unlike the first approach, this one is **not** sequential.

In this approach, bioproductivity is represented by the average rate of electron transfer, experimentally assessable by the rate of O_2 evolution. Two variants of the approach are considered.

12.3.2.1 Single-absorption step model

A simple variant, often used in the literature in fits to performance data of bioreactors, is a single-step excitation model in which the absorption of the required photons is lumped into one step (Eilers & Peeters, 1988, 1993; Han et al., 2000). It is described in the diagram shown in Figure 12.2.

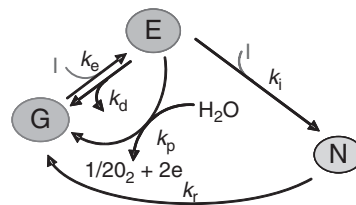


Figure 12.2. Diagram for one-step model (Section 12.3.2.1).

G is the molar fraction of reaction centers in the ground (unexcited) state, E is the molar fraction of excited (catalytically active) centers, and N is the molar fraction of photoinhibited centers. The entities shown near the arrows are rate constants. The sum $E + G + N = 1$ reflects mass conservation. The equations governing these steps are

$$\frac{dG}{dt} = -k_e I G + k_d E + k_p E + k_r N \quad (12.4)$$

$$\frac{dE}{dt} = k_e I G - k_d E - k_p E - k_i E \quad (12.5)$$

$$\frac{dN}{dt} = k_i E - k_r N \quad (12.6)$$

$$\frac{dO_2}{dt} = \frac{1}{2} k_p E \quad (12.7)$$

The following processes affect the rate of change of the ground state (G) fraction:

1. Excitation to the active state owing to the absorption of four photons. Rate constant: $k_e I$, where I is the light intensity (photons hitting a reaction center per second), and k_e is a second-order proportionality constant.
2. Decay of the molecules from the excited state (E). Rate constant $-k_d$.
3. Production process (energy transduction into electron transfer), in which the excited molecule, E , returns to the ground state, G . Rate constant $-k_p$.
4. Recovery of photoinhibited molecules. Rate constant $-k_r$.

The following (pseudo)first-order processes affect the rate of change of the excited state, E :

1. Increase owing to excitation of G . Rate constant $-k_e I$.
2. Decay back to G . Rate constant $-k_d$.
3. Return to G after completing its role in the photosynthetic process. Rate constant $-k_p$.
4. Photoinhibition. Rate constant $-k_i I$.

The following processes affect the rate of change of N :

1. Increase owing to photoinhibition of $E(k_i I)$.
2. Recovery back to $G(k_r)$.

For the sake of simplicity, it is assumed that the coefficients k_e , k_d , k_i , k_p , and k_r are independent of light intensity and culture density.

At low light intensities, in the single-step model, productivity grows linearly with light intensity:

$$\text{Production rate} \propto I \quad (12.8)$$

In Section 12.3.3, it will be shown that this result leads to a contradiction with real reactor biomass production data. The cause for this is the assumption made in Equations 12.4 and 12.5 that the excitation rate of the ground state, G , is linear in the incident light intensity. This is an incorrect assumption, because a linear dependence of light intensity corresponds to the absorption of a **single** photon. In the photosynthetic process, four photons are sequentially absorbed by PS I and an additional four by PS II. Therefore, the excitation rate must be proportional to I^n , with $n \geq 4$, when low intensities are considered. The actual dependence on the light intensity will depend on the details of the photosynthetic mechanism and coupling between the two photosystems.

12.3.2.2 Four-absorption steps model

In the single-step model, it is assumed that all the photons required for the activation of a reaction center are absorbed in one step, which is treated as a rate process. While this might be a reasonable assumption in the case of high light intensity (e.g., at a relatively low culture density), it becomes less obvious when photons are less available as in the case of denser cultures. In order to allow for a more realistic description of light utilization, the absorption of each photon has to be viewed as a separate rate process. Our purpose in this chapter is to provide qualitative features of reactor performance and the role that timescales play in this performance. Therefore, in order to avoid the complexity of a model that takes into account the coupled operation of PS I and PS II, we address the issue of modeling the activity as that of one photosystem. The parameters used in our calculations have been chosen so as to give a good fit to the maximum of measured P-I curves. Hence, it is expected that the model will provide numerical results of the right order of magnitude, though not necessarily identical with actual reactor data.

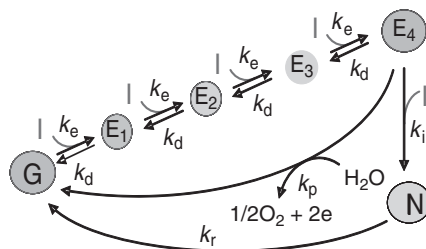


Figure 12.3. Diagram for four-step model (Section 12.3.2.2).

In our model, the ground state, G , is excited in four sequential steps, through four excited states, E_1 , E_2 , E_3 , and E_4 . The last state, E_4 , has the capacity to catalyze electron transfer from water to other electron carriers in the thylakoid membrane, with the formation of O_2 . The model is described in the diagram shown in Figure 12.3.

The rate equations governing the four-step model are:

$$\frac{dG}{dt} = -k_e I G + k_d E_1 + k_p E_4 + k_r N \quad (12.9)$$

$$\left. \begin{aligned} \frac{dE_1}{dt} &= k_e I G + k_d E_2 - k_e I E_1 - k_d E_1, \\ \frac{dE_2}{dt} &= k_e I E_1 + k_d E_3 - k_e I E_2 - k_d E_2, \\ \frac{dE_3}{dt} &= k_e I E_2 + k_d E_4 - k_e I E_3 - k_d E_3, \\ \frac{dE_4}{dt} &= k_e I E_3 - k_i I E_4 - k_p E_4 - k_d E_4 \end{aligned} \right\} \quad (12.10)$$

$$\frac{dN}{dt} = k_i I E_4 - k_r N \quad (12.11)$$

$$\frac{d\text{O}_2}{dt} = \frac{1}{2} k_p E_4 \quad (12.12)$$

In Equations 12.9 and 12.10, all steps share the same excitation parameter, k_e , and the same decay parameter, k_d . However, the parameters may have different values in each of the four steps. The wave functions of different quantum states have different spatial structures, which have the capability of leading to different absorption cross sections. (An example of the effect of such a difference is shown in Figure 12.9.) As knowledge of these parameters is lacking, for the purpose of generating a qualitative picture of the expected effect of the cooperation between the physical motion of the cells and the photosynthetic process, we

have opted for the simple choice given in Equations 12.9 and 12.10.

At low light intensities, in the four-step model, productivity grows nonlinearly with intensity:

$$\text{Production rate} \propto I^4 \quad (12.13)$$

In a more realistic model, which takes into account the existence of two photosystems, the process involves the absorption of eight photons. Hence, depending on the degree of synchronization (or the lack of it) between PS I and PS II, the power in Equation 12.13 may be greater.

12.3.3 One-step versus four-step model

The one-step model has been widely applied in the analysis of biomass production data in reactors in which culture densities and light intensities were low. As the model contains a sufficient number of parameters, reasonable fits to the data may be obtained. However, there are several reservations regarding the use of a one-step model when ultrahigh culture densities and high light intensities are involved:

1. The process is a multi-photon one; four photons have to be absorbed sequentially in order to transfer one electron pair. This leads to Equation 12.13, instead of Equation 12.8.
2. While values of the effective parameters of the one-step model, obtained from fits to low culture density and low light intensity data, may yield a decent fit to the data, they may not correspond to reasonable physiological values. For example, in one such fit, the value found for k_d , the parameter representing the decay of the excited level, is 0.146 s^{-1} (Wu & Merchuk, 2002), corresponding to an average decay time of 7 s. However, the decay times of excited levels in the photosynthetic unit, measured in recent years, vary between nanoseconds to milliseconds (Tyystjärvi & Vass, 2004; Goltsev et al., 2005; Cogdell et al., 2008; Goltsev et al., 2009).
3. The one-step approximation is inappropriate when high culture densities are involved. Consider culture densities that are appreciably higher than the OCD. Then the photic zone is so thin that a reaction center does not manage to collect even a small fraction of the required number of photons in one visit to the photic zone. In fact, it wanders back-and-forth many times across the OP until it manages to collect the photons (with a very small probability). Hence, within a good approximation, the cell is exposed to the **average** of the light intensity across the reactor. Owing to the exponential falloff of

light intensity across the OP, to a good approximation, this average is given by

$$\langle I \rangle \approx \frac{I_0}{\alpha \rho L} \quad (12.14)$$

Here, I_0 is the incident light intensity, α is the specific light attenuation coefficient, and ρ is the culture dry-weight density. Based on Equations 12.8 and 12.13, the production rate per single cell is expected to obey the following proportionality relations:

$$\text{Production rate} \propto \begin{cases} \langle I \rangle \propto \rho^{-1} & \text{One-step} \\ \langle I \rangle^4 \propto \rho^{-4} & \text{Four-step} \end{cases} \quad (12.15)$$

The volumetric production rate is proportional to the product of the single-cell rate multiplied by the culture density, ρ . Consequently, the predictions for the volumetric production rate at extremely high densities in the two models are

$$\begin{aligned} \text{Volumetric production rate} &\propto \\ (\text{Specific production rate}) \times (\text{density}) &\propto \quad (12.16) \\ \begin{cases} \text{Constant} & \text{One-step} \\ \rho^{-3} & \text{Four-step} \end{cases} \end{aligned}$$

The data of volumetric production rates at high densities definitely show that the production rate decreases with culture density and does not go to a constant.

Based on the previous arguments, because of the better qualitative agreement of the four-step model with observations, the remainder of this chapter will focus on the four-step model.

In summary, even such simple qualitative arguments show that **thin-flat plate bioreactors with ultrahigh culture densities probe aspects of algal cell physiology that cannot be tapped in low density, low light intensity reactors.**

12.3.4 Parameter values for Model II

The values of the parameters used in the computations were chosen so as to fit published P-I curves. Otherwise stated, the parameters used in the four-step model will be

$$\begin{aligned} k_e &= 1 \text{ RC photon}^{-1}, & k_d &= 20 \text{ s}^{-1}, & k_p &= 50 \text{ s}^{-1}, \\ k_r &= 0.1 \text{ s}^{-1}, & k_i &= 0.00005 \text{ RC photon}^{-1} \end{aligned} \quad (12.17)$$

12.4 THE IMPORTANCE OF TIMESCALES

12.4.1 Productivity under a flashing light regime

In an average sense, the light regime in high-density flat-plate bioreactors mimics that of light flashes, with randomly varying flash and dark-period durations. In such a situation, the existence of the OCD, the culture density at which the volumetric productivity is maximal, has been interpreted as a result of synchronization between the (average) time a cell spends in the photic zone, and the time necessary to collect the required number of photons (Greenwald, 2010).

The issue of synchronizing the exposure to light with the intrinsic timescales of the photosynthetic process has attracted much attention. Given an incident light intensity, the question of finding the best combination of flash and dark-period durations has preoccupied many researchers (see Phillips & Myers, 1954; Kok, 1956; Lee & Pirt, 1981; Terry, 1986; Tennessen et al., 1995; Matthijs et al., 1996; Nedbal et al., 1996; Shen et al., 1996; Yoshimoto et al., 2005; Gordon & Polle, 2007; Belyaeva et al., 2008; Vejrazka et al., 2011; Xue et al., 2011). However, detailed synchronization could not be attained because the relevant timescales were, and still are, unknown.

To reach a qualitative understanding of the response of an algal culture to the intermittent light regime prevalent in a thin flat-plate bioreactor, we turn, in this section, to the four-step model under the flashing light regime shown in Figure 12.4. The duration of the flash is constant and denoted by Δt_L ; the dark interval between flashes is also fixed and denoted by Δt_D . During a flash, the light intensity, I , is constant.

The response of the catalytic unit to this light regime is obtained by solving Equations 12.9, 12.10, and 12.11 analytically in two stages. The equations are first solved during the light flash (with a constant light intensity, I). They are then solved during the dark interval ($I = 0$). The periodicity of the light regime generates a solution, which tends after a long time toward a periodic one. Namely, the time dependence of G , E_1 , E_2 , E_3 , E_4 , and N tends toward a periodic profile. This periodicity enables one to solve Equations 12.9, 12.10, and 12.11 for the whole cycle

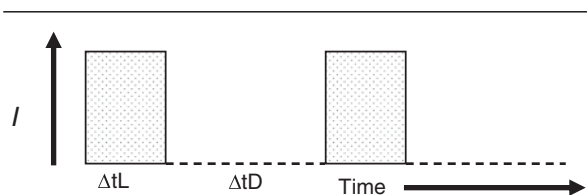


Figure 12.4. Flashing light regime.

completely. The solution for E_4 , the molar fraction of the catalytically active state, is then used in Equation 12.12 to obtain the O_2 evolution rate as a measure of specific productivity.

Figure 12.5 shows the dependence of the long-term average specific production rate on both the flash- and the dark-interval duration. The light intensity on a reaction center has been assigned the value of $1000 \text{ photons s}^{-1}$ (roughly equivalent to one sun). The values of the dark period, Δt_D , vary in the range of 5–200 ms.

$\Delta t_D = 5, 10, \text{ and } 15 \text{ ms}$ are “good” choices because they are of the order of the timescales that characterize the photosynthetic process. We see that as Δt_L , the flash duration, becomes long compared to Δt_D , the duration of the dark interval, the average productivity tends to a constant, which is just the steady-state solution of Equations 12.9, 12.10, 12.11, and 12.12 under continuous illumination. In addition, for obvious reasons, the productivity is higher when the dark period is short. For long dark periods, the approach to the asymptotic constant value requires much longer flash durations.

The values 50, 100, and 200 ms of Δt_D are far too long compared to the timescales of the photosynthetic process and are of the order of the cell’s crossing time of the dark portion of a flat-plate reactor. (For example, in a 1 cm thick reactor, the average crossing time from the middle of the reactor to either side is about 500 ms for a diffusion coefficient, $D = 1 \text{ cm}^2 \text{ s}^{-1}$.) The production rate is much lower than in cycles with Δt_D that is closer to the timescales that characterize the photosynthetic cycle.

To further stress the importance of timescales, we have repeated the calculation, modifying two competing timescales. One timescale, τ_e , is that of the excitation process through the absorption of a photon. It is equal to $1/(k_e I)$. For the values used in Figure 12.5 ($k_e = 1 \text{ RC photon}^{-1}$, and $I = 1000 \text{ photons RC}^{-1} \text{ s}^{-1}$), $\tau_e = 1 \text{ ms}$. The second timescale, τ_d , the timescale for the decay process of an excited state, is given by $(1/k_d)$. For the value used in Figure 12.5 ($k_d = 20 \text{ s}^{-1}$), $\tau_d = 50 \text{ ms}$. Thus, for the parameters used in Figure 12.5, the photon-absorption process is much faster than the decay process.

Reducing the light intensity to $I = 250 \text{ photons RC}^{-1} \text{ s}^{-1}$, the excitation time becomes longer, $\tau_e = 4 \text{ ms}$. However, it is still shorter than the decay timescale (50 ms); hence, one does not expect a dramatic change in the production rate curves. This is seen in Figure 12.6.

The decay timescale, τ_d , used in Figures 12.5 and 12.6 is appreciably longer than experimentally observed timescales of decay processes through which absorbed photon energy is lost. These range from nanoseconds up to

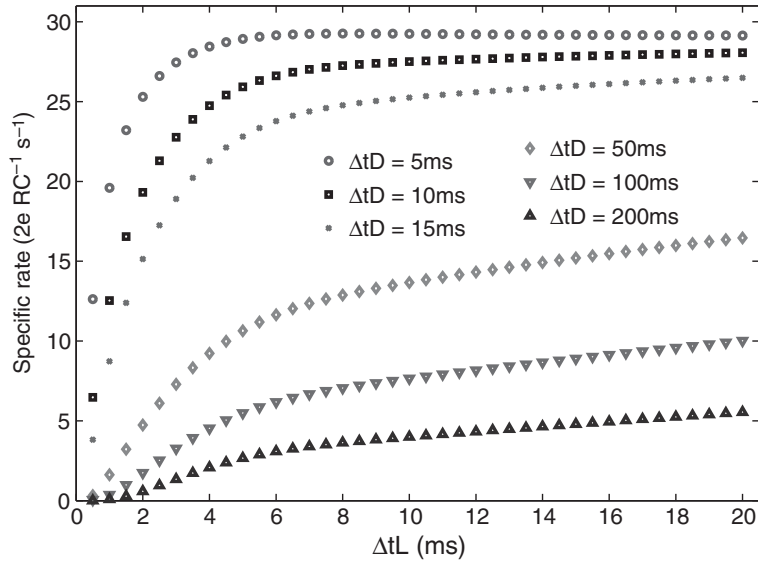


Figure 12.5. Specific rate under a flashing light regime versus flash duration, Δt_L , and dark-period duration, Δt_D , of 5, 10, 15, 50, 100, and 200 ms. Parameters used as in Equation 12.17. Light intensity – $I = 1000$ photons $RC^{-1} s^{-1}$.

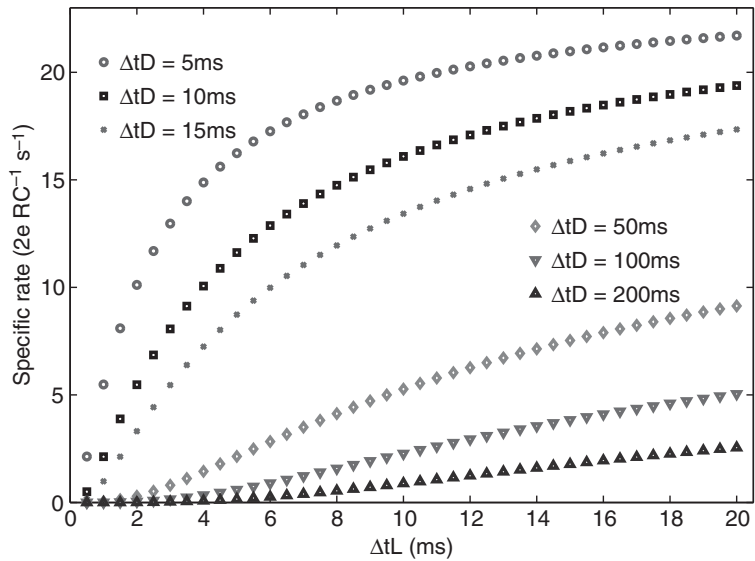


Figure 12.6. Specific rate under a flashing light regime versus flash duration, Δt_L , and dark-period duration, Δt_D , of 5, 10, 15, 50, 100, and 200 ms. Parameters used as in Equation 12.17. Light intensity – $I = 250$ photons $RC^{-1} s^{-1}$.

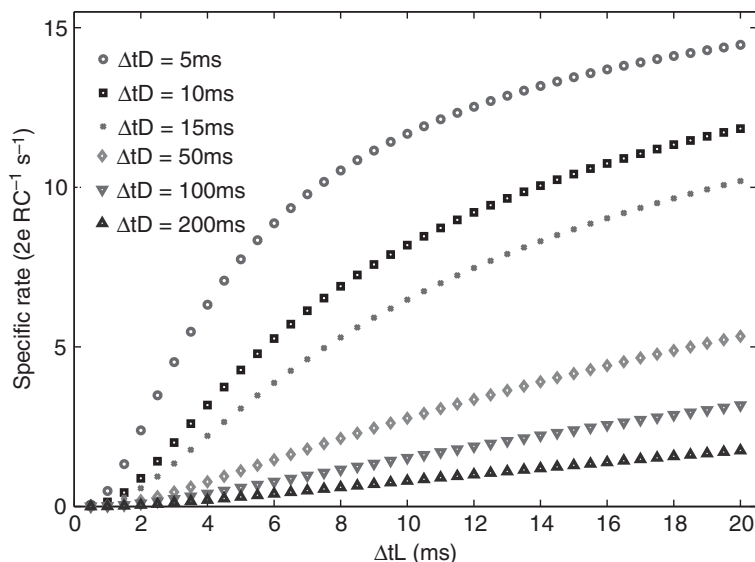


Figure 12.7. Specific rate under a flashing light regime versus flash duration, Δt_L , and dark-period duration, Δt_D , of 5, 10, 15, 50, 100, and 200 ms. Light intensity $-I = 1000$ photons $RC^{-1} s^{-1}$. Parameters given as in Equation 12.17, except for $k_d = 500 s^{-1}$.

several milliseconds (Tyystjärvi & Vass, 2004; Goltsev et al., 2005, 2009; Cogdell et al., 2008). We therefore changed our standard value for k_d to $k_d = 500 s^{-1}$, yielding $\tau_d = 2$ ms, which is closer to the observed timescales. The values for the excitation timescale were, again: $\tau_e = 1$ ms ($I = 1000$ photons s^{-1}) and 4 ms ($I = 250$ photons s^{-1}). The results are shown in Figures 12.7 and 12.8, respectively.

From Figures 12.5, 12.6, and 12.7, one sees that, as long as the excitation timescale is shorter than the decay timescale, the average production rate does not change dramatically. The numbers do change as expected, but are, invariably, of a similar order of magnitude. However, when the decay timescale becomes shorter than the excitation timescale, the production rate is reduced by over an order of magnitude. To show that this situation cannot be remedied by allowing for longer flash durations, we show in Figure 12.8 the results up to $\Delta t_L = 500$ ms. The production rate reaches the steady-state value (corresponding to continuous illumination), but remains appreciably lower than in all other cases for which the excitation timescale was shorter than the decay timescale.

12.4.2 Implications for reactor performance

12.4.2.1 Synchronization at OCD

In thin bioreactors, operating at culture densities around the OCD, synchronization is attained between the time required

for the collection of the required number of photons and the time spent by a cell on average in **one** visit to the photic zone. (This is the analog of Δt_L in the flashing light regime analyzed in Section 12.4.1) This leads to improved performance relative to large OP bioreactors, where no synchronization exists between the timescales of the mechanical motion and those of the photosynthetic apparatus.

12.4.2.2 Time wasted in dark portion of reactor

The time spent in the dark part of a reactor is the equivalent of the dark period between flashes. At high densities, it is far too long compared to physiological timescales. Figures 12.5, 12.6, 12.7, and 12.8 tell us that the productivity is then expected to be lower than what is feasible. The long dark period constitutes wasted time. It therefore calls for a reduction of the OP so as to reduce wasted time.

12.4.2.3 Two-side illumination – effect of timescales

Reduction of the OP below 1 cm is hardly an option owing to mechanical limitations. Another option is illumination of the reactor on both sides. Naively, one might expect that the productivity in a reactor illuminated on both sides will be twice the productivity in one-side illumination. As will be argued in the following, the result depends on the parameter values used in Equations 12.9, 12.10, 12.11, and

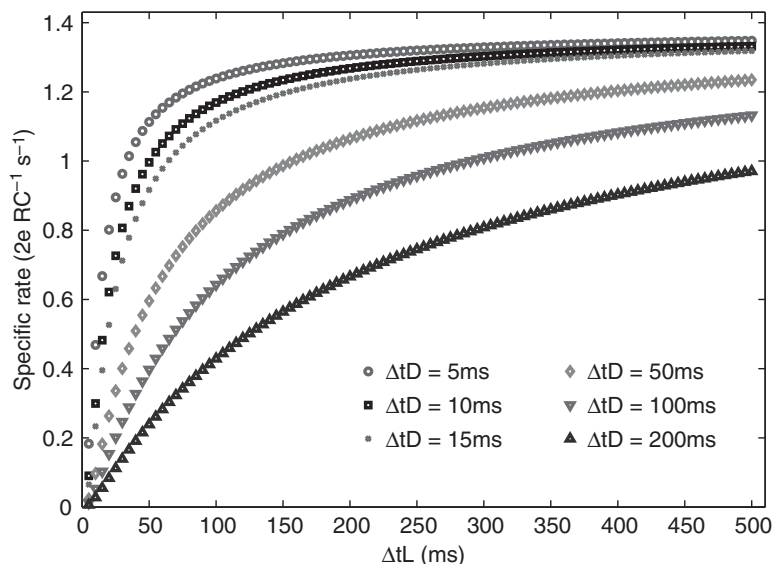


Figure 12.8. Specific rate under a flashing light regime versus flash duration, ΔtL , and dark-period duration, ΔtD , of 5, 10, 15, 50, 100, and 200 ms. Light intensity $-I = 250$ photons $RC^{-1} s^{-1}$. Parameters given as in Equation 12.17, except for $k_d = 500 s^{-1}$.

12.12, which can, again, be translated into timescales. Figures 12.5, 12.6, 12.7, and 12.8 tell us that if the parameter values correspond to a situation in which in every cycle of motion in the reactor (in the average sense, of course) the production rate per cell reaches saturation, one then expects illumination on both sides by the same light intensity to yield twice the volumetric production rate of one-side illumination. The reason is that in two-side illumination, the average time between flashes (motion in the dark portion of the reactor) is half of that time in one-side illumination. If, on the other hand, the parameters correspond to a situation in which the average specific production rate does not reach saturation, then a two-side illumination will yield more than twice the one-side illumination.

12.4.2.4 Flashing light regime reactors

If algal cultures were to be grown under a controlled flashing light regime, in which both the flash duration and the dark period were synchronized with physiological requirements (ΔtL – of the right length to allow for the collection of the required number of photons and ΔtD – synchronized with the duration of the photosynthetic cycle time), then the average production rate might be significantly higher (Gordon & Polle, 2007). Figures 12.5, 12.5, 12.5, and 12.8 provide a demonstration that, to the extent that the results of the four-step model may be viewed as representative of

culture productivity (up to some multiplicative conversion factors and provided the parameters used in the model are consistent with measurements that have not yet been performed), full synchronization may yield a significant improvement in productivity over and above the improvement already achieved in flat-plate bioreactors. Finally, knowledge of the parameters to be used in Equations 12.9, 12.10, and 12.11 is still lacking. Hence, experiments that may shed light on the values of these parameters are in dire need.

12.5 RESULTS OF MODEL CALCULATIONS

12.5.1 Extremely high sensitivity to parameter values

Figures 12.9a and 12.9b show the predictions of the volumetric production rate versus chlorophyll density for two sets of parameter values in the four-step model. The volumetric production rate (units – $mg-DW L^{-1} h^{-1}$) is obtained by multiplying the specific production rate (units – $2e RC^{-1} s^{-1}$) by the chlorophyll density (units – $mg L^{-1}$) and by a conversion factor of 0.16. This factor is based on the following assumptions: chlorophyll/RC ratio is constant and equals 300; and the effective cross section of one reaction center is constant and equals $0.9 nm^2$ (Mauzerall, 1986). These assumptions yield: $mg-Chl = 3.75 nmol RC$; μE

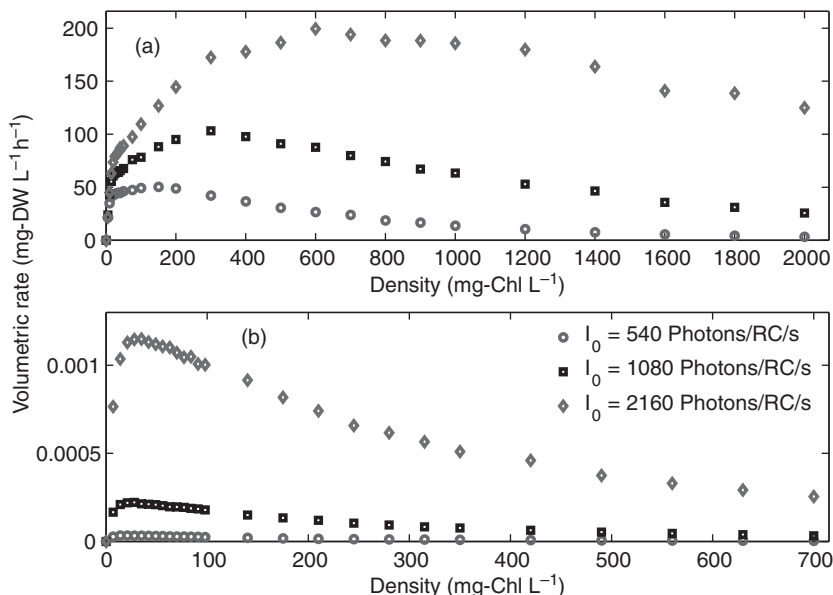


Figure 12.9. Volumetric biomass production rate in four-step version of Model II. Reactor irradiated on one side. Light intensity – 540, 1080, and 2160 photons RC⁻¹ s⁻¹. OP = 1 cm. (a) $k_e = 1$ RC photon⁻¹, $k_d = 20$ s⁻¹, $k_p = 50$ s⁻¹, $k_r = 0.1$ s⁻¹, $k_i = 0.00005$ RC photon⁻¹. (b) Each excitation step has been given a different value for k_e : {1, 0.13, (0.13)², (0.13)³} RC photon⁻¹, $k_d = 200$ s⁻¹, $k_p = 2$ s⁻¹, $k_r = 1/3600$ s⁻¹, $k_i = 0.00001$ RC photon⁻¹.

$m^{-2} s^{-1} = 0.542$ photon RC⁻¹ s⁻¹; and $2e$ RC⁻¹ s⁻¹ = $6.74 \mu\text{mol O}_2/\text{mg-Chl/h}$. In addition, it is assumed that the evolution of 1 mol of oxygen is accompanied by the fixation of 1 mol of carbon (12 g mol^{-1}) and that the carbon content of dry biomass is 50%. The volumetric production rate (units – mg-DW L⁻¹ h⁻¹) is equal to the specific production rate ($2e$ RC⁻¹ s⁻¹) \times density (mg-Chl L⁻¹) \times $6.74 \mu\text{mol O}_2/\text{mg-Chl/h}$ \times $0.012 \text{ mg-C}/\mu\text{mol}$ \times $2 \text{ mg-DW}/\text{mg-C}$.

Parameter values used in Figure 12.9a are given in Equation 12.17. In Figure 12.9b, each excitation step was given a different value for k_c : {1.0, 0.13, (0.13)², (0.13)³} RC photon⁻¹, $k_d = 200$ s⁻¹, $k_p = 2$ s⁻¹, $k_r = 1/3600$ s⁻¹, and $k_i = 0.00001$ RC photon⁻¹. In both figures, incident light intensities are 1000, 2000, and 4000 $\mu\text{mol m}^{-2} \text{ s}^{-1}$ (corresponding to 540, 1080, and 2160 photons RC⁻¹ s⁻¹, respectively). The OP is 1 cm. The enormous difference between the values presented in the two figures shows how important it is to get a good idea of the actual parameter values; these are linked to the timescales of the various steps that partake in the photosynthetic cycle.

12.5.2 No obvious signs of significant photoinhibition as light intensity is raised

For both sets of parameters chosen in Figures 12.9a and 12.9b, the maximal production rate increases by the same

factor as the incident light intensity is raised from the lowest to the highest value. Obviously, the actual increase in the production rate depends crucially on the parameter values assumed. However, the trend is invariably there: at high densities, the production rate increases systematically when light intensity is raised, with no apparent effect of photoinhibition, despite the fact that the photoinhibition mechanism is built in and operative.

12.5.3 Irradiation on one side versus two sides

Figure 12.10 presents a comparison of the volumetric production rate versus the chlorophyll density for a reactor that is illuminated on both sides to twice the production rate of a reactor illuminated only on one side. The light intensity used is 2160 photon s⁻¹ per reaction center (incident intensity of about $4000 \mu\text{mol m}^{-2} \text{ s}^{-1}$). All other parameters are given in Equation 12.17. Again, there is an OCD, corresponding to maximum volumetric productivity. Apart from low densities, there is no discernible difference between the two curves.

This result can be qualitatively understood as follows. The excitation timescale, τ_e , is of the order of $1/(k_e \langle I \rangle)$. With the parameters of Equation 12.17 and the light intensity employed, at high densities, it is roughly 1 ms. The decay timescale, τ_d , ($=1/k_d$) is 50 ms, so that $\tau_d \gg \tau_e$.

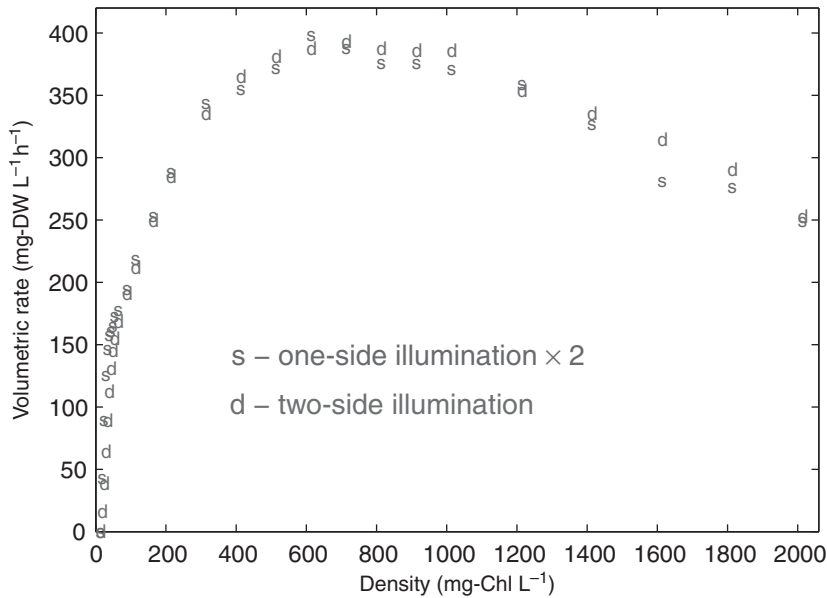


Figure 12.10. Volumetric biomass production rate in four-step version of Model II. Parameter values given as in Equation 12.17. Light intensity – 2160 photons $\text{RC}^{-1} \text{s}^{-1}$. $\text{OP} = 1 \text{ cm}$. d – reactor illuminated on both sides; s – twice production rate in single-side illuminated reactor.

As a result, in every visit to the photic zone, the specific production rate reaches very close to the saturation value of Figure 12.5. The time spent on average in the dark portion of the reactor between consecutive visits at the photic zone in one-side illumination is twice the time spent in the case of two-side illumination case. In each visit, one obtains the same (saturation value) specific production rate, hence, the factor of 2 between the reactor volumetric production rates.

To see the effect of the change in timescales on productivity within our model, we repeated the calculation leading to Figure 12.10 by increasing k_d to 500 s^{-1} (corresponding to $\tau_d = 2 \text{ ms}$). For the same light intensity as above, the qualitative behavior of the result (not shown here) is the same as in Figure 12.10. Namely, the production rate in the two-side illumination case is twice that of the single-side case. Again, the explanation is that one still has τ_e of about 1 ms, which is shorter than $\tau_d (= 2 \text{ ms})$. However, when the incident light intensity is reduced to $250 \mu\text{mol m}^{-2} \text{ s}^{-1}$ (corresponding to $I = 135 \text{ photons RC}^{-1} \text{ s}^{-1}$ on a reaction center) the size relation between the two timescales is reversed. Now $\tau_e \cong 7 \text{ ms}$. The result is that, at low densities, the volumetric production rate in the two-side illumination case is appreciably greater than twice the rate of single-side illumination. This is shown in Figure 12.11.

Again, the result of Figure 12.11 can be understood using qualitative arguments. At high densities, as in the case of Fig. 12.10, the fact that the time spent on average in the dark portion of the collector in one-side illumination is twice the time spent on average in two-side illumination dominates. At very low densities, the whole reactor is illuminated. As the incident illumination becomes very low, the productivity approaches the low intensity limit, where it is proportional to I^4 . At such low radiation levels, the ratio between the productivity in the two-side illumination case and the productivity in the one-side case should approach $2^4 = 16$. While the light intensity used in generating Figure 12.11 is low, it is not low enough to show this limiting behavior, but it does show the transition from the situation in Figure 12.10 to the limiting behavior. Additional calculations (not shown here), in which the incident light intensity hitting a reactor center was lowered to the order of 10 photons s^{-1} , have yielded the limiting ratio of 16.

12.5.4 Results of Model I

Cell random motion plays an extremely important role in reactor performance. It is the cause for the existence of maximal volumetric productivity in the dependence on cell density and/or mixing rate. Within the context of Model I, this fact has been interpreted as evidence (Greenwald,

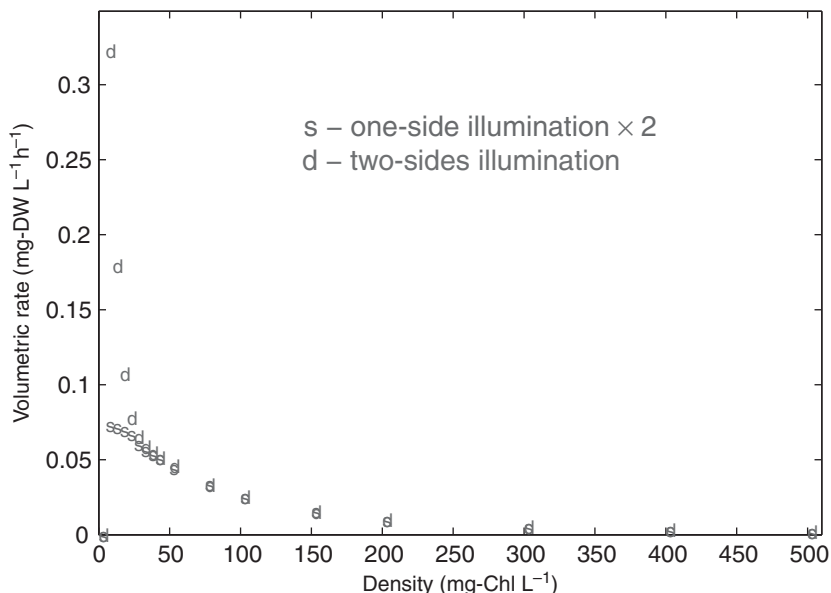


Figure 12.11. Volumetric biomass production rate in four-step version of Model II. Parameter values given as in Equation 12.17, except for $k_d = 500 \text{ s}^{-1}$. Light intensity – 135 photons $\text{RC}^{-1} \text{ s}^{-1}$. $OP = 1 \text{ cm}$. *d* – reactor illuminated on both sides; *s* – twice production rate in single-side illuminated reactor.

2010) that, at the OCD, photon collection in the photic zone attains its highest efficiency. Namely, the time spent in the photic zone is just sufficient for a reaction center to collect the number of photons (8 was the number assumed in calculations) necessary for one photosynthetic cycle. At the OCD, the cell leaves the illuminated layer shortly after having collected the required number of photons. Hence, the chance for photoinhibition owing to being hit by additional photons is reduced significantly, and other cells can enter the photic zone and collect their needed number of photons.

For a **culture density appreciably higher than the OCD**, the photic zone is narrower. Hence, the time spent there becomes shorter. If the incident light intensity is the **same** as that used in the OCD, a reaction center does not have enough time to collect the required photons in one visit and must visit the photic zone more than once. In between visits, it wanders in the dark volume of the reactor and loses some of the photon energy it had just collected owing to decay processes. If, on the other hand, **the culture density is lower than the OCD**, then the photic zone is wider. A cell will then spend more time there than needed to collect the required number of photons. The OCD in the volumetric production rate emerges owing to the rise in productivity at low densities, and its decrease at high densities.

Consider now a reactor operating at an OCD of 10 g L^{-1} . Most of the volume of the reactor is virtually in complete darkness. Assuming an attenuation coefficient of $1 \text{ L g}^{-1} \text{ cm}^{-1}$, the illuminated layer (“photic” zone) is about 1 mm thick. For a diffusion coefficient, D , of about $1 \text{ cm}^2 \text{ s}^{-1}$, the time spent by a cell in this layer from the moment it enters the layer until it leaves it for the first time (the “first passage time” (see, Gardiner, 2009)) is of the order of 10 ms. For this time span to be sufficient for the collection of 8 photons, the reaction center has to be exposed to photons at a rate of $800 \text{ photons s}^{-1}$. For a photosystem with effective cross-section area of 5 nm^2 , this corresponds to a photon flux of $1.6 \times 10^{20} \text{ photons m}^{-2} \text{ s}^{-1}$, which is about $270 \text{ } \mu\text{mol m}^{-2} \text{ s}^{-1}$. This is the average light intensity in the photic zone, corresponding roughly to an incident light intensity of $430 \text{ } \mu\text{mol m}^{-2} \text{ s}^{-1}$. If, however, the OCD is 20 g L^{-1} , then the thickness of the photic zone is about 0.5 mm, and the “first passage time” is of the order of 3 ms. Collection of eight photons within this time span requires an incident radiation of about $1200 \text{ } \mu\text{mol m}^{-2} \text{ s}^{-1}$. Clearly, if the values of the diffusion coefficient, D , or the effective cross-section area were different from the ones used above, then the resulting numbers would have been different. Still, the regularity is obvious: **random cell motion yields a specific increase of the OCD as radiation intensity is raised.**

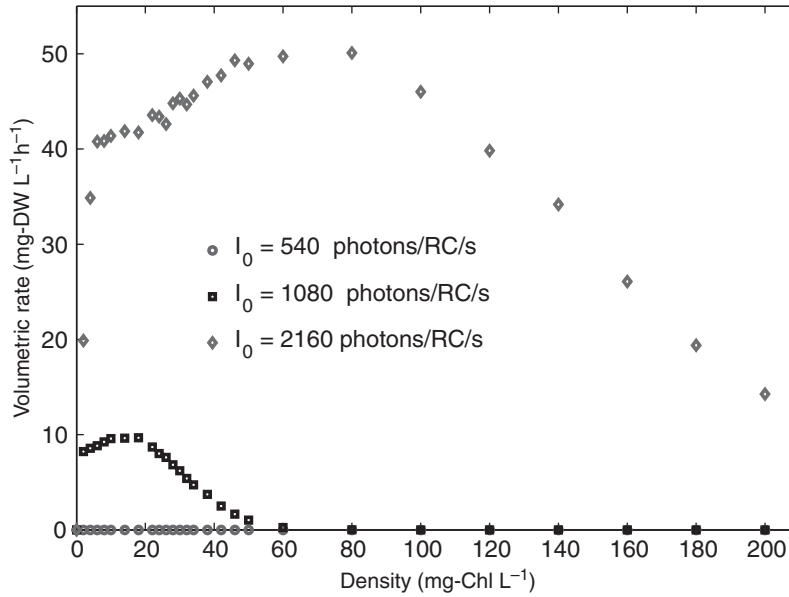


Figure 12.12. Volumetric biomass production rate in Model I. Reactor irradiated on one side. $T_d = T_e = 10$ ms. Light intensity – 540, 1080, and 2160 photons $\text{RC}^{-1} \text{s}^{-1}$. $\text{OP} = 1$ cm.

A detailed study (Greenwald, 2010), using tools of the theory of random process as applied to the motion of algal cells, yields the following prediction:

$$\text{OCD} = K\sqrt{I_0} \quad (12.18)$$

Here, I_0 is the incident light intensity. The existing data (Hu et al., 1998a, 1998b) are consistent with Equation 12.18. Moreover, the coefficient, K , allows for an estimate of the diffusion coefficient, D , which controls random cell motion, to be $0.2\text{--}2 \text{ cm}^2 \text{ s}^{-1}$. The marvelous finding is that **this estimate is consistent with an estimate based on pure hydrodynamic theory (Sato & Seguchi, 1975, 1981) which has nothing to do with bioreactors!**

Figure 12.12 shows an example of the qualitative behavior expected in Model I. The timescales used T_d (“digestion” period during which a reaction center that has collected the required number of photons, 8 assumed here, is unavailable for absorbing additional impinging photons) and T_e (timescale for photon energy loss) are $T_d = T_e = 10$ ms. The calculation yields the number of photosynthetic cycles completed on average by a reaction center per second. The conversion factor to the volumetric production rate is the same as in Section 12.5.1. The trend is similar to that observed in the results of the four-step model: there is an OCD, corresponding to a maximal volumetric production rate; productivity grows significantly when the incident light intensity is raised.

The result of Figure 12.12 demonstrates again the significance of timescales. In the lowest light intensity (540 photons $\text{RC}^{-1} \text{ s}^{-1}$), the time to collect 8 photons is higher than $8/540$ s, which is close to 15 ms. The timescale for photon energy loss is shorter, 10 ms. Consequently, the reaction center can **never** collect the required number of photons (8). At most, it can collect 5.4 photons. Hence, it does not manage to complete even one photosynthetic cycle. To allow for nonvanishing productivity in this model, the light intensity must exceed 800 photons $\text{RC}^{-1} \text{ s}^{-1}$. Of course, in a realistic system, things are never as sharp. However, this result indicates that when the light intensity is sufficiently low, the mere effect of photon energy losses may hinder productivity.

In summary, the qualitative characteristics that emerge in both Figures 12.9a and 12.9b (Model II, different parameters) and Model I are the same:

1. The volumetric production rate has a maximum.
2. Productivity consistently increases as light intensity is raised, with no obvious signs of photoinhibition.

12.6 OPEN QUESTIONS

The ideas and numerical results presented in this chapter raise several questions regarding both our understanding of the fluid dynamical aspects that are responsible for the

random motion of the cells and the quantitative aspects of the **dynamics** of the photosynthetic process.

12.6.1 Physical aspects

12.6.1.1 Bubble-induced turbulence

There is no satisfactory theory for the turbulent flow induced in a fluid owing to the passage of air bubbles. Only a phenomenological description exists, based on approximations and containing unknown parameters, which have been determined empirically (Sato & Seguchi, 1975, 1981). In particular, there is no solid understanding of edge effects for motion close to the reactor walls.

12.6.1.2 Dependence of physical parameters on culture density

The highest culture densities studied did not exceed 10 g L⁻¹, constituting less than a 10% change in the specific weight of the whole culture (fluid + algae). Depending on the alga species, even such a small percentage may affect fluid properties such as viscosity. This may be relevant in particular in the case of *S. platensis*, where algal cells combine in groups of 10–100 cells into spirals of lengths and diameters of 50–1000 and 5–8 μm, respectively. It has been observed that, when colloidal structures of similar sizes are in suspension in a fluid in similar concentrations, they have an observable effect on viscosity (Bolhouse, 2010), which may have a direct effect, for example, on the effective diffusion coefficient, *D*. In fact, the data of Hu et al. (1998a) for the cultivation of *S. platensis* in thin flat-plate bioreactors indicate that the effective diffusion coefficient may have a weak dependence on culture density.

12.6.2 Dynamical aspects of photosynthesis

The models discussed in this review indicate that the random motion of cells plays a dominant role in reactor productivity; it enables an increase in productivity, significantly above that of conventional bioreactors by allowing synchronization between the average timescales of the physical motion of algae cells and those of the photosynthetic process. Qualitatively, the experimental trends are reproduced. However, it is obvious that at present one is not in a position to provide numerical predictions that can be compared in a quantitative manner with experimental results.

12.6.2.1 Rate constants/timescales

The timescales in Model I and the rate constants in Model II are not known. At best, one has some notion of their order of magnitude. For example, in the four-step model, physical considerations indicate that k_e (the proportionality

constant in $k_e I$, the rate constant for excitation by photon absorption) and k_d (the rate constant for photon energy loss by decay) need not have the same value in the ground state and the four excited states. Their determination for each of the states may require the employment of techniques developed in the last two decades in the physical sciences for measuring the characteristics of quantum systems over very short timescales.

Another example is the value of k_i , the proportionality constant in $k_i I$, the rate constant for photoinhibition. Based on carefully designed experiments, it has been found that the value of k_i corresponds to one photoinhibition event roughly every 10⁷ photons (Baroli & Melis, 1996; Tyystjärvi & Aro, 1996). This low probability of photoinhibition does not seem to be consistent with the fact that small amounts of very dilute cultures tend to die within a few hours even if exposed to a small fraction of one sun. One possible explanation is that the empirically found value for k_i is affected by two density-shading effects. First, an experiment is performed in a culture. The light intensity falls off through the culture, and, hence the actual light intensity, to which cells are exposed is an average of the exponentially falling intensity. This may cause a certain reduction in the calculated value of k_i . Probably, a much greater effect may be generated by mutual shading of chlorophyll antennae within a cell because these are arranged not just on the surface of a cell, but in layers of some thickness. The combined effect of both effects of light attenuation may lead to a determination of an **effective** k_i , which is 10–100 smaller than the value that ought to be used in the rate equations for a single reaction center.

12.6.2.2 Light absorption within a cell

The previous point implies that better models for light absorption by antennae organized on the thylakoid membranes are needed.

12.6.2.3 Acclimation to flash-light regime synchronized with physiological timescales

There is a wealth of information regarding the acclimation of algae to light regimes under **continuous illumination**, both concerning production rates as well as modification of cellular chlorophyll content (Torzillo et al., 2005). Under continuous illumination, when light intensity is high, there is a tendency to reduce antennae size, and when it is low, the tendency is to increase antennae area. These trends can be understood as a tendency of cells to increase the efficiency of photon collection under low illumination conditions, and to minimize photoinhibition under high light intensities.

As mentioned in Section 12.4, there is extensive literature on the response of algae to exposure to light flashes. However, the flash durations as well as dark intervals did not necessarily correspond to **synchronization** with the short timescales that characterize the photosynthetic process because the latter were, and are still, unknown. Furthermore, there is no detailed information regarding the **long-term** acclimation of algae to such a light regime.

Consider a situation in which cells are exposed to light with flash durations that are **just** sufficient for collecting the required number of photons (say, 8), so that the effect of photoinhibition is minimized, and the dark intervals between flashes are synchronized with the “digestion” period, during which a reaction center is busy converting photon energy into chemical energy and is not available for the exploitation of additional photons. Then, there need not be any advantage in modifying the antennae area when the light intensity is raised, or lowered, if concurrently, the length of the light flash is modified so that it is sufficient for the absorption of the required number of photons and no more! We certainly do not know what happens under such conditions. If, by chance, cells are “indifferent” to light intensities under the correctly synchronized flash duration, then it may be beneficial to genetically engineer cells to have antennae areas that are advantageous for other reasons. Section 12.4 provides an example for the need to synchronize the flash duration and the dark interval between flashes with the timescales that characterize the photosynthetic cycle.

REFERENCES

- Al Issa, S. & Lucas, D. (2009) Two phase flow 1D turbulence model for poly-disperse upward flow in a vertical pipe. *Nucl. Eng. Design* 239: 1933–1943.
- Baroli, I. & Melis, A. (1996) Photoinhibition and repair in *Dunaliella salina* acclimated to different growth irradiances. *Planta* 198: 640–646.
- Belyaeva, N.E., Schmitt, F.-J., Steffen, R., Paschenko, V.Z., Riznichenko, G.Y., Chemeris, Y.K., Renger, G. & Rubin, A.B. (2008) PS II model-based simulations of single turnover flash-induced transients of fluorescence yield monitored within the time domain of 100 ns–100 s on dark adapted *Chlorella pyrenoidosa* cells. *Photosynth. Res.* 98: 105–119.
- Bolhouse, A.M. (2010) Rheology of algae slurries. MSc thesis, University of Texas at Austin.
- Cogdell, R.J., Gardiner, A.T., Hashimoto, H. & Brotsudarmo, T.H. (2008) A comparative look at the first few milliseconds of the light reactions of photosynthesis. *Photochem. Photobiol. Sci.* 7: 1150–1158.
- Deen, N.G., Solberg, T. & Hjertager, B.H. (2001) Large eddy simulation of the gas–liquid flow in a square cross-sectioned bubble column. *Chem. Eng. Sci.* 56: 6341–6349.
- Dubinsky, Z., Falkowski, P.G. & Wyman, K. (1986) Light harvesting and utilization by phytoplankton. *Plant Cell Physiol.* 27: 1335–1349.
- Eilers, P.H.C. & Peeters, J.H.C. (1988) A model for the relationship between light intensity and the rate of photosynthesis in phytoplankton. *Ecol. Model.* 42: 199–221.
- Eilers, P.H.C. & Peeters, J.H.C. (1993) Dynamic behavior of a model for photosynthesis and photoinhibition. *Ecol. Model.* 69: 113–133.
- Falkowski, P.G., Owens, T.G., Ley, A.C. & Mauzerall, D.C. (1981) Effects of growth irradiance levels on the ratio of reaction centers in two species of marine phytoplankton. *Plant Physiol.* 68: 969–973.
- Falkowski, P.G., Dubinsky, Z. & Wyman, K. (1985) Growth-irradiance relationships in phytoplankton. *Limnol. Oceanogr.* 30: 311–321.
- Gardiner, C.W. (2009) *Stochastic Methods: A Handbook for the Natural and Social Sciences*. Springer Verlag, New York.
- Gebremariam, A.K. (2008) Analyzing the effect of motion of algae cells in ultrahigh dense cultures on biomass productivity. MSc thesis, Ben-Gurion University of the Negev.
- Gebremariam, A.K. & Zarmi, Y. (2012) Synchronization of fluid-dynamics related and physiological time scales and algal biomass production in thin flat-plate bioreactors. *J. Appl. Phys.* 111(3): 034904.
- Gitelson, A., Hu, Q. & Richmond, A. (1996) Photic volume in photo-bioreactors supporting ultrahigh population densities of the photoautotroph *Spirulina platensis*. *Appl. Environ. Microbiol.* 62: 1570–1573.
- Goltsev, V., Chernev, P., Zaharieva, I., Lambrev, P. & Strasser, R.J. (2005) Kinetics of delayed chlorophyll *a* fluorescence registered in milliseconds time range. *Photosynth. Res.* 84: 209–215.
- Goltsev, V., Zaharieva, I., Chernev, P. & Strasser, R.J. (2009) Delayed fluorescence in photosynthesis. *Photosynth. Res.* 101: 217–232.
- Gordon, J.M. & Polle, J.E.W. (2007) Ultrahigh bioproductivity from algae. *Appl. Microbiol. Biotechnol.* 76: 969–975.
- Greenwald, E. (2010) A stochastic model of algal photo-bioreactors. MSc thesis, Ben-Gurion University of the Negev.
- Han, B.P., Virtanen, M., Koponen, J. & Straskraba, M. (2000) Effect of photoinhibition on algal photosynthesis: a dynamic model. *J. Plankton Res.* 22: 865–885.
- Hu, Q., Guterman, H. & Richmond, A. (1996) Physiological characteristics of *Spirulina platensis* (Cyanobacteria) cultured at ultrahigh cell densities. *J. Phycol.* 32: 1066–1073.
- Hu, Q., Kurano, N., Kawachi, M., Iwasaki, I. & Miyachi, S. (1998a) Ultrahigh-cell-density culture of a marine green alga *Chlorococcum littorale* in a flat-plate photo-bioreactor. *Appl. Microbiol. Biotechnol.* 49: 655–662.

- Hu, Q., Zarmi, Y. & Richmond, A. (1998b) Combined effects of light intensity, light-path and culture density on output rate of *Spirulina platensis* (Cyanobacteria). *Eur. J. Phycol.* 33: 165–171.
- Kok, B. (1956) Photosynthesis in flashing light. *Biochim. Biophys. Acta* 21: 245–258.
- Lee, Y.-K. & Pirt, S.J. (1981) Energetics of photosynthetic algal growth: influence of intermittent illumination in short (40 s) cycles. *J. Gen. Microbiol.* 124: 43–52.
- Matthijs, H.C.P., Balke, H., Van Hes, U.M., Kroon, B.M., Mur, L.R. & Binot, R.A. (1996) Application of light-emitting diodes in bioreactors: flashing light effects and energy economy in algal culture (*Chlorella pyrenoidosa*). *Biotechnol. Bioeng.* 50: 98–107.
- Mauzerall, D. (1986) The optical cross section and absolute size of a photosynthetic unit. *Photosynth. Res.* 10: 163–170.
- Michiyoshi, I. & Serizawa, A. (1986) Turbulence in two-phase bubbly flow. *Nucl. Eng. Design* 95: 253–267.
- Nedbal, L., Tichy, V., Xiong F. & Grobbelaar, J.U. (1996) Microscopic green algae and cyanobacteria in high-frequency intermittent light. *J. Phycol.* 8: 325–333.
- Pan, Y., Dudukovic, M.P. & Chang, M. (1999) Dynamic simulation of bubbly flow in bubble columns. *Chem. Eng. Sci.* 54: 2481–2489.
- Pfleger, D., Gomes, S., Gilbert, N. & Wagner, H.-G. (1999) Hydrodynamic simulations of laboratory scale bubble columns fundamental studies of the Eulerian–Eulerian modeling approach. *Chem. Eng. Sci.* 54: 5091–5099.
- Phillips, J.N. & Myers, J. (1954) Growth rate of *Chlorella* in flashing light. *Plant Physiol.* 29: 152–161.
- Richmond, A. (1996) Efficient utilization of high irradiance for production of photoautotrophic cell mass: a survey. *J. Appl. Phycol.* 8: 381–387.
- Richmond, A. (2000) Microalgal biotechnology at the turn of the millennium: a personal view. *J. Appl. Phycol.* 12: 441–451.
- Richmond, A. (2003) Growth characteristics of ultrahigh-density microalgal cultures. *Biotechnol. Bioprocess Eng.* 8: 349–353.
- Richmond, A. (2004a) Biological principles of mass cultivation. In: *Handbook of Microalgal Culture: Biotechnology and Applied Phycology* (ed. A. Richmond), pp. 125–177, Blackwell Science, Oxford.
- Richmond, A. (2004) Principles for attaining maximal microalgal productivity in photo-bioreactors: an overview. *Hydrobiologia* 512: 33–37.
- Richmond, A. & Hu, Q. (1997) Principles for efficient utilization of light for mass production of photoautotrophic microorganisms. *Appl. Biochem. Biotechnol.* 63–65: 649–658.
- Richmond, A. & Zou, N. (1999) Efficient utilization of high photon irradiance for mass production of photoautotrophic microorganisms. *J. Appl. Phycol.* 11: 123–127.
- Richmond, A. & Zhang, C.W. (2001) Optimization of a flat plate glass reactor for mass production of *Nannochloropsis* sp. outdoors. *J. Biotechnol.* 85: 259–269.
- Richmond, A., Lichtenberg, E., Stahl, B. & Vonshak, A. (1990) Quantitative assessment of the major limitations on productivity of *Spirulina platensis* in open raceways. *J. Appl. Phycol.* 2: 195–206.
- Richmond, A., Zhang, C.W. & Zarmi, Y. (2003) Efficient use of strong light for high photosynthetic productivity: interrelationships between the optical path, the optimal population density and cell-growth inhibition. *Biomol. Eng.* 20: 229–236.
- Sato, Y. & Sekoguchi, K. (1975) Liquid velocity distribution in two-phase bubble flow. *Int. J. Multiphase Flow* 2: 79–95.
- Sato, Y. & Sekoguchi, K. (1981) Momentum and heat transfer in two-phase flow-I theory. *Int. J. Multiphase Flow* 7: 167–177; see also 179–190.
- Schenk, P.M., Thomas-Hall, S.R., Stephens, E., Marx, U.C., Mussgnug, J.H., Posten, C., Kruse, O. & Hankamer, B. (2008) Second generation biofuels: high-efficiency microalgae for biodiesel production. *Bioenerg. Res.* 1: 20–43.
- Shen, Y.K., Chow, W.S. & Park, Y.I. (1996) Photo-inactivation of photosystem II by cumulative exposure to short light pulses during the induction period of photosynthesis. *Photosynth. Res.* 47: 51–59.
- Sokolichin, A., Eigenberger, G. & Lapin, A. (2004) Simulation of buoyancy driven bubbly flow: established simplifications and open questions. *AIChE J.* 50: 24–45.
- Sukenik, A., Levy, R.S., Levy, Y., Falkowski, P.G. & Dubinsky, Z. (1991) Optimizing algal biomass production in an outdoor pond: a simulation model. *J. Appl. Phycol.* 3: 191–201.
- Tennessen, D.J., Bula, R.J. & Sharkey, T.D. (1995) Efficiency of photosynthesis in continuous and pulsed light emitting diode irradiation. *Photosynth. Res.* 44: 261–269.
- Terry, K.L. (1986) Photosynthesis in modulated light: quantitative dependence of photosynthetic enhancement on flashing rate. *Biotechnol. Bioeng.* 28: 988–995.
- Torzillo, G., Göksan, T., Isik, O. & Gökpinar, S. (2005) Photon irradiance required to support optimal growth and interrelations between irradiance and pigment composition in the green alga *Haematococcus pluvialis*. *Eur. J. Phycol.* 40: 233–240.
- Tyystjärvi, E. & Aro, E.M. (1996) The rate constant of photoinhibition, measured in lincomycin-treated leaves, is directly proportional to light intensity. *Proc. Nat. Acad. Sci. USA* 93: 2213–2218.
- Tyystjärvi, E. & Vass, I. (2004) Light emission as a probe of charge separation and recombination in the photosynthetic apparatus. In: *Chlorophyll a Fluorescence: A Signature of Photosynthesis* (ed. G.C. Papageorgiou), pp. 363–388. Springer, Amsterdam.

- Vejrazka, C., Janssen, M., Streefland, M. & Wijffels, R.H. (2011) Photosynthetic efficiency of *Chlamydomonas reinhardtii* in flashing light. *Biotechnol. Bioeng.* 108: 2905–2913.
- Wu, X. & Merchuk, J.C. (2002) Simulation of algae growth in a bench-scale bubble column reactor. *Biotechnol. Bioeng.* 80: 156–168.
- Xue, S., Su, Z. & Cong, W. (2011) Growth of *Spirulina platensis* enhanced under intermittent illumination. *J. Biotechnol.* 151: 271–277.
- Yoshimoto, N., Sato, T. & Kondo, Y. (2005) Dynamic discrete model of flashing light effect in photosynthesis of microalgae. *J. Appl. Phycol.* 17: 207–214.
- Zou, N. & Richmond A. (1999) Effect of light-path length in outdoor flat plate reactors on output rate of cell mass and of EPA in *Nannochloropsis* sp. *J. Biotechnol.* 70: 351–356.
- Zou, N. & Richmond, A. (2000) Light-path length and population density in photo-acclimation of *Nannochloropsis* sp. (Eustigmatophyceae). *J. Appl. Phycol.* 12: 349–354.